MOX–Report No. 14/2010

A Mimetic Discretization of Elliptic Obstacle Problems

Paola F. Antonietti, Lourenco Beirão da Veiga,
Marco Verani

MOX, Dipartimento di Matematica "F. Brioschi"
Politecnico di Milano, Via Bonardi 9 - 20133 Milano (Italy)

mox@mate.polimi.it http://mox.polimi.it

A Mimetic Discretization of Elliptic Obstacle Problems*

Paola F. Antonietti[a], Lourenco Beirão da Veiga[b] and Marco Verani[a]

3th, May 2010

[a] MOX, Dipartimento di Matematica, Politecnico di Milano, Piazza Leonardo da Vinci 32, I-20133 Milano, Italy
paola.antonietti@polimi.it, marco.verani@polimi.it

[b] Dipartimento di Matematica, Università di Milano, Via Saldini 50, I-20133 Milano, Italy.
lourenco.beirao@unimi.it

Abstract

We develop a Finite Element method (FEM) which can adopt very general meshes with polygonal elements for the numerical approximation of elliptic obstacle problems. This kind of methods are also known as mimetic discretization schemes, which stem from the Mimetic Finite Difference (MFD) method. The first-order convergence estimate in a suitable (mesh-dependent) energy norm is established. Numerical experiments confirming the theoretical results are also presented.

Keywords: Mimetic Finite Difference Methods, obstacle problem.
2000 Mathematics Subject Classification. Primary 65N30; Secondary 35R35.

1 Introduction

Elliptic obstacle problems refer to find the equilibrium position of an elastic membrane whose boundary is held fixed, and which is constrained to lie above a given obstacle. It can be considered as a model problem for variational inequalities (see, e.g, [20]), and it has found applications in a number of different fields as elasticity and fluid dynamics. For example, applications include fluid filtration in porous media, optimal control, and financial mathematics [23, 22].

In the present paper we develop, for the obstacle problem, a low order Finite Element Method (FEM) which can adopt very general meshes. This kind of meshes are made of (possibly non convex) polygons of variable number of edges, and do not have to fulfill matching conditions. This type of schemes, which stem from the Mimetic Finite Difference (MFD) method, are nowadays known also as mimetic discretization methods. The first papers introducing an interpretation of the Mimetic Finite Difference method

*The first and the third authors were supported in part by the Italian research project PRIN 2008: *"Analysis and development of advanced numerical methods for PDEs"*

as a generalization of the Finite Element Method are very recent [11, 13]. Lately, this generalization of FEM has been applied to a wide range of problems, a very short list including [9, 12, 3, 14, 2, 26, 4, 1, 25].

The rest of the paper is organized as follows. In Section 2 we introduce the model problem, and fix some notations. The Mimetic Finite Difference method is introduced in Section 3, and the convergence analysis is provided in Section 4. Finally, in Section 5 we discuss some implementation issues, and in Section 6 we show some numerical results.

2 The obstacle problem

Throughout the paper we will use standard notations for Sobolev spaces, norms and seminorms. For a bounded domain D in $\mathbb{R}^d$, $d = 1, 2$, we denote by $H^s(D)$ the standard Sobolev space of order $s \geq 0$, and by $\|\cdot\|_{H^s(D)}$ and $|\cdot|_{H^s(D)}$ the usual Sobolev norm and seminorm, respectively. For $s = 0$, we write $L^2(D)$ in lieu of $H^0(D)$. $H_0^1(D)$ is the subspace of $H^1(D)$ of functions with zero trace on ∂D.

Let Ω be an open, bounded, convex set of $\mathbb{R}^2$, with either a polygonal or a C^2-smooth boundary $\Gamma := \partial\Omega$. Let $g := \tilde{g}_{|\Gamma}$, with $\tilde{g} \in H^2(\Omega)$ and we set

$$V^g := \{v \in H^1(\Omega) : \quad v = g \text{ on } \Gamma\}.$$

Let us introduce the bilinear form $a(u, v) : V^g \times V^g \longrightarrow \mathbb{R}$ defined by

$$a(u, v) := \int_\Omega \nabla u \cdot \nabla v \, \mathrm{d}x,$$

and the linear functional $F(v) : V^g \longrightarrow \mathbb{R}$ with

$$F(v) := \int_\Omega f \; v \, \mathrm{d}x,$$

where we assume $f \in L^2(\Omega)$. Let us introduce the function $\psi \in H^2(\Omega)$ with $\psi \leq g$ on Γ and the convex space

$$K := \{v \in V^g \; : \; v \geq \psi \text{ a.e. in } \Omega\}.$$

We are interested in solving the following variational inequality:

$$\begin{cases} \text{Find } u \in K \text{ such that} \\ a(u, v - u) \geq F(v - u) \qquad \forall v \in K. \end{cases} \tag{2.1}$$

It is well known [8] that under the above data regularity assumption, the elliptic obstacle problem (2.1) admits a unique solution $u \in H^2(\Omega)$.

3 A mimetic discretization

In this section we present a mimetic discretization method for the obstacle problem (2.1). This method is the direct extension of the scheme presented in [9] for the problem without obstacle.

3.1 Mesh notation and assumptions

Let $\Omega_h \subset \Omega$ be a polygonal approximation of Ω, in such a way that all vertexes of Ω_h which are on the boundary of Ω_h are also on the boundary of Ω. The polygonal domain Ω_h represents the computational domain for the method. With a little abuse of notation, we also denote by Ω_h a partition of the above introduced computational domain into polygons E. We assume that this partition is conformal, *i.e.*, intersection of two different elements E_1 and E_2 is either a few mesh points, or a few mesh edges (two adjacent elements may share more than one edge) or empty. We allow Ω_h to contain non-convex and degenerate elements. For each polygon E, k_E denotes its number of vertexes, $|E|$ denotes its area, h_E denotes its diameter and

$$h := \max_{E \in \Omega_h} h_E.$$

We denote the set of mesh vertexes and edges by $\mathcal{N}_h$ and $\mathcal{E}_h$, the set of internal vertexes and edges by $\mathcal{N}_h^0$ and $\mathcal{E}_h^0$, the set of boundary vertexes and edges by $\mathcal{N}_h^\partial$ and $\mathcal{E}_h^\partial$. The set of vertexes and edges of a particular element E are denoted by $\mathcal{N}_h^E$ and $\mathcal{E}_h^E$, respectively. Moreover, we denote a generic mesh vertex by v, a generic edge by e and its length both by h_e and $|\mathsf{e}|$. A fixed orientation is also set for the mesh Ω_h, which is reflected by a unit normal vector $\mathbf{n}_\mathsf{e}$, $\mathsf{e} \in \mathcal{E}_h$, fixed once for all. For every polygon E and edge $\mathsf{e} \in \mathcal{E}_h^E$, we define a unit normal vector $\mathbf{n}_E^\mathsf{e}$ that points outside E.

The mesh is assumed to satisfy the following shape regularity properties, which have already been used in [9]. There exist

- an integer number N_s independent of h;
- a real positive number ρ independent of h;
- a *compatible* sub-decomposition $\mathcal{T}_h$ of every Ω_h into shape-regular triangles,

such that

(H1) any polygon $E \in \Omega_h$ admits a decomposition $\mathcal{T}_h|_E$ formed by less than N_s triangles;

(H2) any triangle $T \in \mathcal{T}_h$ is shape-regular in the sense that the ratio between the radius r of the inscribed ball and the diameter h_T of T is bounded from below by ρ:

$$0 < \rho \leq \frac{r}{h_T}.$$

From (H1), (H2) there can be easily derived the following useful properties that we list below.

(M1) The number of vertexes and edges of every polygon E of Ω_h are *uniformly* bounded from above by two integer numbers N_v and N_e, which only depend on N_s.

(M2) There exists a real positive number σ_s, which only depends on N_s and ρ, such that

$$h_{\mathsf{e}} \geq \sigma_s h_E \qquad \text{and} \qquad |E| \geq \sigma_s h_E^2,$$

for every polygon E of every decomposition Ω_h, and for every edge e of E.

(M3) There exists a constant C_a, only dependent on ρ and N_s, such that for every polygon E, for every edge e of E and for every function $\psi \in H^1(E)$ it holds the *trace inequality*:

$$\|\psi\|^2_{L^2(\mathsf{e})} \leq C_a\Big(h_E^{-1}\|\psi\|^2_{L^2(E)} + h_E\,|\psi|^2_{H^1(E)}\Big). \tag{3.1}$$

(M4) There exists a constant C_{app}, which is independent of h, such that the following holds. For every E and for every function $\psi \in H^m(E)$, $m \in \mathbb{N}$, there exists a polynomial ψ_k of degree k living on E such that

$$|\psi - \psi_0|_{H^l(E)} \leq C_{app} h_E^{m-l}\,|\psi|_{H^m(E)}$$

for all integers $0 \leq l \leq m \leq k+1$.

Note that (M4) follows, for instance, from the extended Bramble-Hilbert lemma on non star-shaped domains of [17, 6].

3.2 Degrees of freedom and interpolation operators

The discretization of problem (2.1) requires to discretize a scalar field in $H^1(\Omega)$. In order to do so, we start introducing the degrees of freedom for the discrete approximation space. The discrete space V_h is defined as follows: a vector $v_h \in V_h$ consists of a collection of degrees of freedom

$$v_h := \{v^{\mathsf{v}}\}_{\mathsf{v}\in\mathcal{N}_h},$$

one per internal mesh vertex, *e.g.* to every vertex $\mathsf{v} \in \mathcal{N}_h$, we associate a real number v^{v}. The scalar v^{v} represents the nodal value of the underlying discrete scalar field of displacement. The number of unknowns is equal to the number of vertexes of the mesh. We also define the discrete space $V_h^g \subset V_h$ of functions which satisfy the Dirichlet boundary conditions

$$V_h^g := \{v_h \in V_h \ : \ v_h^{\mathsf{v}} = g(\mathsf{v})\ \forall \mathsf{v} \in \mathcal{N}_h^{\partial}\}\ .$$

Accordingly, V_h^0 represents the space of discrete functions which vanish at the boundary nodes.

We define the following interpolation operator from the spaces of smooth enough functions to the discrete space V_h. For every function $v \in \mathcal{C}^0(\bar{\Omega}) \cap H^1(\Omega)$, we define $v_{\mathrm{I}} \in V_h$ by

$$v_{\mathrm{I}}^{\mathsf{v}} := v(\mathsf{v}) \quad \forall \mathsf{v} \in \mathcal{N}_h.$$

Moreover, we analogously define the local interpolation operator from $\mathcal{C}^0(\bar{E}) \cap H^1(E)$ into $V_h|_E$ given by

$$v_{\mathrm{I}}^{\mathsf{v}} := v(\mathsf{v}) \quad \forall \mathsf{v} \in \mathcal{N}_h^E.$$

3.3 Discrete norms and bilinear forms

We endow the space V_h with the following discrete seminorm

$$\|v_h\|_{1,h}^2 := \sum_{E\in\Omega_h} \|v_h\|_{1,h,E}^2 = \sum_{E\in\Omega_h} |E| \sum_{\mathsf{e}\in\mathcal{E}_h^E} \left[\frac{1}{|\mathsf{e}|}(v^{\mathsf{v}_2} - v^{\mathsf{v}_1})\right]^2, \tag{3.2}$$

where v_1 and v_2 are the two vertexes of e. The quantity $\|\cdot\|_{1,h}$ is a $H^1(\Omega)$-type discrete seminorm, which becomes a norm on V_h^0. Indeed, the differences $\frac{1}{|\mathsf{e}|}(v^{\mathsf{v}_2} - v^{\mathsf{v}_1})$ represent gradients on edges and the scalings with respect to h_E and h_{e} are the correct ones to mimic an $H^1(E)$ local seminorm. In the numerical tests we will also consider the following $L^2(\Omega)$- and $L^\infty(\Omega)$-type discrete norms

$$\begin{aligned} \|v_h\|_{0,h}^2 &:= \sum_{E\in\Omega_h} |E| \sum_{\mathsf{v}\in\mathcal{N}_h^E} (v^{\mathsf{v}})^2 \\ \|v_h\|_{\infty,h} &:= \max_{\mathsf{v}\in\mathcal{N}_h} |v^{\mathsf{v}}|. \end{aligned} \tag{3.3}$$

We denote by $a_h(\cdot,\cdot) : V_h \times V_h \to \mathbb{R}$ the discretization of the bilinear form $a(\cdot,\cdot)$, defined as follows:

$$a_h(v_h, w_h) := \sum_{E\in\Omega_h} a_h^E(v_h, w_h) \quad \forall v_h, w_h \in V_h, \tag{3.4}$$

where $a_h^E(\cdot,\cdot)$ is a symmetric bilinear form on each element E. The local forms mimick

$$a_h^E(v_h, w_h) \sim \int_E \nabla\widetilde{v}_h \cdot \nabla\widetilde{w}_h \,\mathrm{d}x,$$

where, roughly speaking, $\widetilde{v}_h, \widetilde{w}_h$ denote regular functions living on E which "extend the data" v_h, w_h inside the element.

We introduce two fundamental assumptions for the local bilinear form $a_h^E(\cdot,\cdot)$. The first one represents the coercivity (up to the kernel) and the correct scaling with respect to the element size.

(S1) There exist two positive constants c_1 and c_2 independent of h such that, for every $u_h, v_h \in V_h$ and each $E \in \Omega_h$, we have

$$c_1\|v_h\|_{1,h,E}^2 \le a_h^E(v_h, v_h), \qquad a_h^E(u_h, v_h) \le c_2\|u_h\|_{1,h,E}\|v_h\|_{1,h,E}.$$

In order to introduce the second assumption, we observe beforehand that, using an integration by parts,

$$\begin{aligned} \int_E \nabla v \cdot \nabla p^1 \,\mathrm{d}x &= -\int_E (\Delta p^1) v \,\mathrm{d}x + \sum_{\mathsf{e}\in\mathcal{E}_h^E} \int_{\mathsf{e}} (\nabla p^1 \cdot \mathbf{n}_E^{\mathsf{e}}) v \,\mathrm{d}s \\ &= \sum_{\mathsf{e}\in\mathcal{E}_h^E} \nabla p^1 \cdot \mathbf{n}_E^{\mathsf{e}} \int_{\mathsf{e}} v \,\mathrm{d}s \end{aligned} \tag{3.5}$$

for all $E \in \Omega_h$, for all $v \in [H^1(E)]^2$ and for all linear functions p^1. By substituting the integral in the last term of (3.5) with a trapezium integration rule gives our second condition.

(S2) For every element E, every linear vector function p^1 on E, and every $v_h \in V_h$, it holds

$$a_h^E(v_h, (p^1)_I) = \sum_{\mathsf{e} \in \mathcal{E}_h^E} (\nabla p^1 \cdot \mathbf{n}_E^{\mathsf{e}}) \frac{|\mathsf{e}|}{2} \big(v_h^{\mathsf{v}_1} + v_h^{\mathsf{v}_2}\big), \tag{3.6}$$

where v_1 and v_2 are the two vertexes of $\mathsf{e} \in \mathbf{n}_E^{\mathsf{e}}$.

The meaning of the above consistency condition (S2) is therefore that the discrete bilinear form respects integration by parts when tested with linear functions.

Remark 3.1. *The scalar product and the bilinear form shown in this section can be easily built element by element in a simple algebraic way. A brief description of such construction can be found in Section 5.*

3.4 The discrete method

Finally, we are able to define the proposed mimetic discrete method for the obstacle problem. Let the loading term

$$(f, v_h)_h := \sum_{E \in \Omega_h} \bar{f}|_E \sum_{i=1}^{k_E} v^{\mathsf{v}_i} \omega_E^i, \tag{3.7}$$

where $\mathsf{v}_1, \ldots, \mathsf{v}_{k_E}$ are the vertexes of E, $\bar{f}|_E := \frac{1}{|E|} \int_E f \, \mathrm{d}x$, and $\omega_E^1, \ldots, \omega_E^{k_E}$ are positive weights such that $\sum_{i=1}^{k_E} \omega_E^i = |E|$. The above loading term is an approximation of

$$(f, v_h)_h \sim \int_\Omega f \tilde{v}_h \, \mathrm{d}x,$$

which is exact for constant functions.

Let us introduce the convex space

$$K_h := \{v_h \in V_h^g \ : \ v_h^{\mathsf{v}} \geq \psi(\mathsf{v}) \ \forall \mathsf{v} \in \mathcal{N}_h\}.$$

Then, the mimetic discretization of problem (2.1) reads:

$$\begin{cases} \text{Find } u_h \in K_h \text{ such that} \\ a_h(u_h, v_h - u_h) \geq (f, v_h - u_h)_h \qquad \forall v_h \in K_h. \end{cases} \tag{3.8}$$

Due to property (S1) it is immediate to check that the bilinear form $a_h(\cdot, \cdot)$ is coercive on $V_h/\mathbb{R}$. As a consequence, recalling again that $K_h \subset V_h$ is convex and closed, standard results [15] give the existence and uniqueness of a solution for the discrete problem (3.8). The uniform stability of the problem with respect to h will be left as an implicit consequence of the analysis that follows.

4 Convergence of the method

In this section we prove the linear convergence of the proposed discrete method. In the following, we will use the symbols $\simeq$, $\lesssim$, $\gtrsim$ to represent equivalences and bounds which hold up to a constant independent of the mesh-size.

4.1 A lifting operator

In this section we show that, for all $E \in \Omega_h$, there exists a suitable lifting operator

$$R_h^E \,:\, V_h|_E \longrightarrow H^1(E) \cap \mathcal{C}^0(\bar{E}),$$

which satisfies the following properties.

(L1) $(R_h^E v_h)(\mathsf{v}) = v_h^{\mathsf{v}} \quad \forall \mathsf{v} \in \mathcal{N}_h^E$ and $\forall v_h \in V_h|_E$;

(L2) $R_h^E v_h|_{\mathsf{e}}$ is a linear function $\forall \mathsf{e} \in \mathcal{E}_h^E$ and $\forall v_h \in V_h|_E$;

(L3) $R_h^E(p^1)_{\mathrm{I}} = p^1$ for all linear functions p^1 on E;

(L4) $|R_h^E v_h|^2_{H^1(E)} \lesssim \|v_h\|^2_{1,h,E} \quad \forall v_h \in V_h|_E$;

(L5) $\|R_h^E v_{\mathrm{I}}\|^2_{L^2(E)} \lesssim \sum_{k=0}^{2} h_E^{2k} |v|^2_{H^k(E)} \quad \forall v \in H^2(E)$;

(L6) The following maximum principle holds: for all $v_h \in V_h|_E$, if $v_h^{\mathsf{v}} \geq 0 \; \forall \mathsf{v} \in \mathcal{N}_h^E$ then the lifting operator satisfies $R_h^E v_h \geq 0$ in E.

Note that, due to properties (L1) and (L2), the global lifting operator

$$\begin{aligned} &R_h \,:\, V_h \longrightarrow H^1(\Omega_h) \cap \mathcal{C}^0(\bar{\Omega}_h)\,, \\ &R_h(v_h)|_E := R_h^E(v_h|_E) \quad \forall v_h \in V_h,\; E \in \Omega_h, \end{aligned}$$

is well defined.

The local lifting operator is built as in [5], which in turn is an improved version of that presented in [9]. Note that we cannot directly use the lifting operator of [9] since it does not preserve linear functions. Let $E \in \Omega_h$, for a given $v_h \in V_h|_E$, the function $R_h^E v_h$ is globally continuous and piecewise linear on the sub-triangulation $\mathcal{T}_h$ and it is defined in the following way. On the vertexes $\mathsf{v} \in \mathcal{N}_h^E$ we set $R_h^E v_h(\mathsf{v}) = v_h^{\mathsf{v}}$. On the remaining nodes of $\mathcal{T}_h$ that lay on the boundary, $R_h^E v_h$ is defined by linear interpolation of the two vertex values of the edge. On the internal nodes of E, we do instead the following construction. Given any internal node v of $\mathcal{T}_h$, we call Ξ_{v} the set of nodes which share an edge with v and are different from v. Then, it is easy to check that v, which lays in the convex hull determined by the nodes $\{\bar{\mathsf{v}}\}_{\bar{\mathsf{v}} \in \Xi_{\mathsf{v}}}$, can be expressed (in a non unique way) as a weighted sum

$$\mathsf{v} = \sum_{\bar{\mathsf{v}} \in \Xi_{\mathsf{v}}} w_{\bar{\mathsf{v}}}^{\mathsf{v}}\, \bar{\mathsf{v}}, \tag{4.1}$$

with $w_{\mathsf{v}}^{\mathsf{v}}$ non-negative real numbers such that $\sum_{\bar{\mathsf{v}}\in\Xi_{\mathsf{v}}} w_{\mathsf{v}}^{\mathsf{v}} = 1$. For each internal node v, we then enforce the condition

$$R_h^E v_h(\mathsf{v}) - \sum_{\bar{\mathsf{v}}\in\Xi_{\mathsf{v}}} w_{\mathsf{v}}^{\mathsf{v}}\, R_h^E v_h(\bar{\mathsf{v}}) = 0\ . \tag{4.2}$$

This set of conditions provides a square linear system which determines the value of $R_h^E v_h$ in the internal nodes. Indeed, it is immediate to verify that the associated matrix is an M-matrix, which in particular implies the existence of a unique solution and a discrete maximum principle. Therefore, assumption (L6) is satisfied.

Properties (L1) and (L2) are clearly satisfied by construction. Furthermore, following the same argument as in [9], from the maximum principle it follows that the operator R_h^E satisfies also the stability condition (L4). We now check property (L3). Let p_1 be a linear function on E. Since the solution of the linear system introduced above is unique, in order to show $R_h^E(p^1)_{\mathrm{I}} = p^1$ it is sufficient to prove that p_1 satisfies (4.2) for any v internal node of E. Using (4.1) and recalling that p_1 is linear, it holds

$$p_1(\mathsf{v}) = p_1(\sum_{\bar{\mathsf{v}}\in\Xi_{\mathsf{v}}} w_{\mathsf{v}}^{\mathsf{v}}\,\bar{\mathsf{v}}) = \sum_{\bar{\mathsf{v}}\in\Xi_{\mathsf{v}}} w_{\mathsf{v}}^{\mathsf{v}}\, p_1(\bar{\mathsf{v}})$$

for all the internal nodes v of E, which is exactly (4.2) for the function p_1.

We are left to show property (L5). We start observing that, due to the maximum principle,

$$\|R_h^E v_I\|_{L^\infty(E)} \le \max_{\mathsf{v}\in\mathcal{N}_h^E} |v_I^{\mathsf{v}}| = \max_{\mathsf{v}\in\mathcal{N}_h^E} |v(\mathsf{v})| \le \|v\|_{L^\infty(E)}. \tag{4.3}$$

Moreover, due to (H1) and (H2) it is easy to check that

$$h_E \lesssim h_T \le h_E \quad \forall T \in \mathcal{T}_h|_E. \tag{4.4}$$

Using (4.3), a scaling argument on each triangle of $T \in \mathcal{T}_h|_E$, and finally (4.4), we get

$$\begin{aligned} \|R_h^E v_I\|_{L^2(E)}^2 &\le |E| \|v\|_{L^\infty(E)}^2 = |E| \max_{T\in\mathcal{T}_h} \|v\|_{L^\infty(T)}^2 \\ &\le |E| \max_{T\in\mathcal{T}_h} \sum_{k=0}^{2} h_T^{2k-2} |v|_{H^k(T)}^2 \lesssim |E| \sum_{k=0}^{2} h_E^{2k-2} |v|_{H^k(E)}^2\ . \end{aligned} \tag{4.5}$$

Property (L5) follows from the above bound and $|E| \le h_E^2$. This completes the proof of properties (L1)-(L6).

Finally, we make the following two observations. Given any $E \in \Omega_h$ and $v \in H^2(E)$, let v_1 be its linear approximation introduced in (M4) setting $k = 1$. Then, using (L3), (L5), and finally the approximation property (M4) we get

$$\begin{aligned} \|v - R_h^E v_{\mathrm{I}}\|_{L^2(E)}^2 &\lesssim \|v - v_1\|_{L^2(E)}^2 + \|R_h^E (v_1 - v)_{\mathrm{I}}\|_{L^2(E)}^2 \\ &\lesssim \sum_{k=0}^{2} h_E^{2k} |v - v_1|_{H^k(E)}^2 \lesssim h_E^4\, |v|_{H^2(E)}^2 \end{aligned} \tag{4.6}$$

for all $E \in \Omega_h$. Furthermore, due to the maximum principle property (L6) and the definition (3.2) of discrete H^1-norm it follows

$$\|R_h^E v_h - v_h^{\mathsf{v}}\|_{L^\infty(E)} \leq \max_{\mathsf{v}' \in \mathcal{N}_h^E} |v_h^{\mathsf{v}'} - v_h^{\mathsf{v}}| \lesssim \|v_h\|_{1,h} \ ,$$

which also gives immediately

$$\|R_h^E v_h - v_h^{\mathsf{v}}\|_{L^2(E)} \lesssim h_E \|v_h\|_{1,h} \ . \tag{4.7}$$

4.2 A convergence result

In this section, we prove a convergence result for the mimetic discretization method applied to the variational inequality (2.1). The proof takes the steps from [10].

Theorem 4.1. *Let $u \in K \cap H^2(\Omega)$ be the solution to the continuous problem (2.1), and $u_h \in K_h$ be the corresponding mimetic approximation, obtained by solving the discrete problem (3.8). Then, it holds*

$$\|u_h - u_I\|_{1,h} \leq Ch,$$

where the constant C is independent of the mesh-size h.

Proof. We set $e_h := u_h - u_{\mathrm{I}}$ and $u^1 := I^1 u$, where I^1 is the Lagrangian interpolation operator onto the space of continuous piecewise linear functions defined on Ω_h. We observe that, due to (L2), it holds

$$\frac{|\mathsf{e}|}{2}\left(e_h^{\mathsf{v}_1} + e_h^{\mathsf{v}_2}\right) = \int_{\mathsf{e}} R_h^E e_h \, \mathrm{d}x \quad \forall E \in \Omega_h, \mathsf{e} \in \mathcal{E}_h^E \ .$$

By using (S1)-(S2), the discrete problem (3.8), and the above observation we get

$$\begin{aligned} c_1 \|e_h\|_{1,h}^2 \leq & a_h(e_h, e_h) \\ \leq & (f, e_h)_h - a_h(u_{\mathrm{I}}, e_h) \\ = & (f, e_h)_h - a_h(u_{\mathrm{I}} - (u^1)_{\mathrm{I}}, e_h) - a_h((u^1)_{\mathrm{I}}, e_h) \\ \leq & (f, e_h)_h + c_2 \|u_{\mathrm{I}} - (u^1)_{\mathrm{I}}\|_{1,h} \|e_h\|_{1,h} - \sum_{E \in \Omega_h} \sum_{\mathsf{e} \in \mathcal{E}_h^E} \frac{\partial u^1}{\partial \mathbf{n}_E^{\mathsf{e}}} \int_e R_h^E e_h \, \mathrm{d}x \ . \end{aligned} \tag{4.8}$$

From (4.8), using twice an integration by parts and that $R_h e_h$ vanishes on the boundary

of Ω_h, it follows

$$\begin{aligned}
c_1\|e_h\|_{1,h}^2 &\le (f,e_h)_h + c_2\|u_{\mathrm{I}} - (u^1)_{\mathrm{I}}\|_{1,h}\|e_h\|_{1,h} - \sum_{E\in\Omega_h}\int_E \nabla R_h^E e_h\cdot\nabla u^1\,\mathrm{d}x\\
&= (f,e_h)_h + c_2\|u_{\mathrm{I}} - (u^1)_{\mathrm{I}}\|_{1,h}\|e_h\|_{1,h} + \sum_{E\in\Omega_h}\int_E \nabla R_h^E e_h\cdot\nabla (u-u^1)\,\mathrm{d}x\\
&\quad - \sum_{E\in\Omega_h}\int_E \nabla R_h^E e_h\cdot\nabla u\,\mathrm{d}x\\
&= (f,e_h)_h + c_2\|u_{\mathrm{I}} - (u^1)_{\mathrm{I}}\|_{1,h}\|e_h\|_{1,h} + \sum_{E\in\Omega_h}\int_E \nabla R_h^E e_h\cdot\nabla (u-u^1)\,\mathrm{d}x\\
&\quad + \int_{\Omega_h}\Delta u\; R_h^E e_h\,\mathrm{d}x.
\end{aligned}$$

Let us preliminary estimate the term $\|u_{\mathrm{I}} - (u^1)_{\mathrm{I}}\|_{1,h} \equiv \|(u-u^1)_{\mathrm{I}}\|_{1,h}$. For simplicity, we set $v = u - u^1$. Using definition (3.2) of the norm $\|\cdot\|_{1,h}$ and the Cauchy-Schwarz inequality, we get

$$\begin{aligned}
\|v_{\mathrm{I}}\|_{1,h}^2 &= \sum_{E\in\Omega_h}|E|\sum_{\mathsf{e}\in\mathcal{E}_h^E}\left[\frac{1}{|\mathsf{e}|}\left(v^{\mathsf{v}_2} - v^{\mathsf{v}_1}\right)\right]^2 = \sum_{E\in\Omega_h}|E|\sum_{\mathsf{e}\in\mathcal{E}_h^E}\left[\frac{1}{|\mathsf{e}|}\int_e v'\,\mathrm{d}s\right]^2\\
&\le \sum_{E\in\Omega_h}|E|\sum_{\mathsf{e}\in\mathcal{E}_h^E}\left[\frac{1}{|\mathsf{e}|}\|\nabla v\|_{L^2(\mathsf{e})}^2\right].
\end{aligned}$$

Applying the trace inequality (3.1) to ∇v and employing a standard interpolation error estimate yield

$$\|(u-u^1)_{\mathrm{I}}\|_{1,h}^2 \lesssim \sum_{E\in\Omega_h}\left[\|\nabla(u-u^1)\|_{L^2(E)}^2 + h_E^2\,|u|_{H^2(E)}^2\right] \lesssim h^2\,|u|_{H^2(\Omega)}^2\,. \tag{4.9}$$

From (4.2), by employing the Young inequality combined with (4.9) and introducing $w = \Delta u + f$, we get

$$\|e_h\|_{1,h}^2 \lesssim \left\{(f,e_h)_h - \int_{\Omega_h} f\; R_h e_h\,\mathrm{d}x\right\} + h^2\,|u|_{H^2(\Omega)}^2 \tag{4.10}$$

$$+ \sum_{E\in\Omega_h}\int_E \nabla R_h^E e_h\cdot\nabla(u-u^1)\,\mathrm{d}x + \int_{\Omega_h} w\; R_h^E e_h\,\mathrm{d}x. \tag{4.11}$$

As shown in [7], there holds

$$w \le 0 \quad \text{and} \quad w(\psi - u) = 0 \qquad \text{a.e. in } \Omega_h. \tag{4.12}$$

Simply adding and subtracting terms, we obtain

$$\begin{aligned}
\int_{\Omega_h} w R_h^E e_h\,\mathrm{d}x &= -\int_{\Omega_h} w(R_h^E u_{\mathrm{I}} - u)\,\mathrm{d}x + \int_{\Omega_h} w(\psi - u)\,\mathrm{d}x\\
&\quad + \int_{\Omega_h} w(R_h^E u_h - R_h^E\psi_{\mathrm{I}})\,\mathrm{d}x + \int_{\Omega_h} w(R_h^E\psi_{\mathrm{I}} - \psi)\,\mathrm{d}x.
\end{aligned} \tag{4.13}$$

The second term in the right hand side of (4.13) vanishes due to (4.12). Moreover, as for every $\mathsf{v} \in \mathcal{N}_h$ there holds $u_h(\mathsf{v}) \geq \psi_{\mathrm{I}}(\mathsf{v})$, employing assumption (L6) yields

$$R_h^E u_h - R_h^E \psi_{\mathrm{I}} \geq 0 \quad \text{in } \Omega_h,$$

which recalling (4.12) gives $\int_{\Omega_h} w(R_h^E u_h - R_h^E \psi_{\mathrm{I}})\,\mathrm{d}x \leq 0$. Hence, combining this last two observations with (4.13), we get

$$\int_{\Omega_h} w R_h^E e_h \,\mathrm{d}x \leq \int_{\Omega_h} w(u - R_h^E u_{\mathrm{I}})\,\mathrm{d}x + \int_{\Omega_h} w(R_h^E \psi_{\mathrm{I}} - \psi)\,\mathrm{d}x.$$

The above bound, using the Cauchy-Schwarz inequality, (4.6), and recalling that $w = \Delta u + f$, yields

$$\int_{\Omega_h} w R_h^E e_h \,\mathrm{d}x \lesssim h^2 \|w\|_{L^2(\Omega_h)} \Big(|\psi|_{H^2(\Omega_h)} + |u|_{H^2(\Omega_h)} \Big) \lesssim h^2. \tag{4.14}$$

We now estimate the remaining pieces in (4.10). By using (4.7) and proceeding as in the estimate of the *First Piece* in [9], it is easy to check that there holds

$$\big|(f, e_h)_h - (f, R_h^E e_h)\big| \lesssim h \|f\|_{L^2(\Omega)} \|e_h\|_{1,h} \lesssim h \|e_h\|_{1,h}. \tag{4.15}$$

Using the Cauchy-Schwarz inequality, assumption (L4) and a standard interpolation error estimate yields

$$\begin{aligned} \sum_{E \in \Omega_h} \int_E \nabla R_h^E e_h \cdot \nabla(u - u^1)\,\mathrm{d}x &\leq \|\nabla R_h^E e_h\|_{L^2(\Omega_h)} \|\nabla(u - u^1)\|_{L^2(\Omega_h)} \\ &\lesssim h \|e_h\|_{1,h}\, |u|_{H^2} \lesssim h \|e_h\|_{1,h}\ . \end{aligned} \tag{4.16}$$

Combining (4.10) with (4.14), (4.15) and (4.16) finally gives

$$\|e_h\|_{1,h}^2 \lesssim h \|e_h\|_{1,h} + h^2,$$

which immediately gives the result. □

Remark 4.1. *The convexity condition on Ω can be relaxed to include a more general class of domains, provided that the solution u still belongs to $H^2(\Omega)$, and Ω_h can be inscribed in Ω for every h (*e.g.*, non-convex polygonal domains). Indeed, repeating the same argument, the convergence result still holds.*

Remark 4.2. *Whenever V^g coincide with $H_0^1(\Omega)$,* i.e.*, homogeneous boundary conditions are imposed on the domain boundary, Theorem 4.1 can be proved in a much simpler way, following the idea proposed in [19]. We refer to Appendix A. for the details.*

5 Implementation issues

In this section we show briefly how the local scalar product appearing in (3.4) is built in practice. Let E be a general element of Ω_h, with $k_E \geq 3$ vertexes. Then, we need to build an $k_E \times k_E$ symmetric matrix M which represents the local scalar product

$$a_h^E(v_h, w_h) = v_h^T \mathsf{M}\, w_h \qquad \forall\, v_h, w_h \in \mathbb{R}^{k_E} \ .$$

Let the functions $\rho_1 := 1, \rho_2 := x - \bar{x}, \rho_3 := y - \bar{y}$ represent a basis for the space of the linear polynomials on E, with x, y cartesian coordinates in the plane and $(\bar{x}, \bar{y})$ representing the position of the center of mass of E. Then, we introduce the $k_E \times 3$ matrix N given by

$$\mathsf{N}(i,j) := \rho_j(\mathsf{v}_i) \qquad i = 1, \ldots, k_E,\ j = 1, 2, 3 \ ,$$

where $\mathsf{v}_1 = (x_1, y_1), \ldots, \mathsf{v}_{k_E} = (x_{k_E}, y_{k_E})$ are the k_E vertexes of the polygon E, *i.e.*,

$$\mathsf{N} := \begin{pmatrix} 1 & x_1 - \bar{x} & y_1 - \bar{y} \\ 1 & x_2 - \bar{x} & y_2 - \bar{y} \\ 1 & x_3 - \bar{x} & y_3 - \bar{y} \\ \vdots & \vdots & \\ 1 & x_{k_E} - \bar{x} & y_{k_E} - \bar{y} \end{pmatrix} . \tag{5.1}$$

Then, it is easy to check that the consistency condition (S2) can be expressed as

$$v_h^T \mathsf{M}\mathsf{N} = v_h^T \mathsf{R} \quad \forall v_h \in \mathbb{R}^{k_E} \ ,$$

where the $k_E \times 3$ matrix $\mathbb{R}$ with columns $\mathsf{R}_{|j}$, $j = 1, 2, 3$, is the unique matrix that represents the right hand side of (S2)

$$v_h^T \mathsf{R}_{|j} = \sum_{\mathsf{e} \in \mathcal{E}_h^E} (\nabla \rho_j \cdot \mathbf{n}_E^{\mathsf{e}}) \frac{|\mathsf{e}|}{2} \big(v_h^{\mathsf{v}_1} + v_h^{\mathsf{v}_2} \big) \quad \forall v_h \in \mathbb{R}^{k_E} \ .$$

More precisely, for $i = 1, \ldots, k_E$, let e_i be the edge connecting the vertexes $\mathsf{v}_i = (x_i, y_i)$ and $\mathsf{v}_{i+1} = (x_{i+1}, y_{i+1})$ (with the convention that $\mathsf{v}_{k_E+1} \equiv \mathsf{v}_1$), and let $\mathbf{n}_E^{\mathsf{e}_i} \in \mathbf{R}^{1\times 2}$ be the corresponding outward unit normal vector. Clearly, $\mathbf{n}_E^{\mathsf{e}_i} = (y_{i+1} - y_i, x_i - x_{i+1})$. Therefore, the matrix R has the following form

$$\mathsf{R} = \begin{pmatrix} 0 & (\mathbf{n}_E^{\mathsf{e}_{k_E}} + \mathbf{n}_E^{\mathsf{e}_1})/2 \\ 0 & (\mathbf{n}_E^{\mathsf{e}_1} + \mathbf{n}_E^{\mathsf{e}_2})/2 \\ 0 & (\mathbf{n}_E^{\mathsf{e}_2} + \mathbf{n}_E^{\mathsf{e}_3})/2 \\ \vdots & \vdots \\ 0 & (\mathbf{n}_E^{\mathsf{e}_{k_E-1}} + \mathbf{n}_E^{\mathsf{e}_{k_E}})/2 \end{pmatrix} = \begin{pmatrix} 0 & (y_2 - y_{k_E})/2 & (x_{k_E} - x_2)/2 \\ 0 & (y_3 - y_1)/2 & (x_1 - x_3)/2 \\ 0 & (y_4 - y_2)/2 & (x_2 - x_4)/2 \\ \vdots & \vdots & \vdots \\ 0 & (y_1 - y_{k_E-1})/2 & (x_{k_E-1} - x_1)/2 \end{pmatrix} , \tag{5.2}$$

and the consistency condition can be written as

$$\mathsf{M}\mathsf{N} = \mathsf{R} \ , \tag{5.3}$$

where the matrices N, R are given in (5.1) and (5.2), respectively. Moreover, it is easy to check that

$$(\mathsf{R}^T\mathsf{N})(i,j) = (\mathsf{N}^T\mathsf{M}\mathsf{N})(i,j) = \int_E \nabla\rho_i \cdot \nabla\rho_j \,\mathrm{d}x =: \mathsf{K}(i,j) \quad i,j = 1,2,3\ , \tag{5.4}$$

with $\mathsf{K}(i,j)$ clearly equal to $|E|$ if $i = j = 2$ or $i = j = 3$ and zero otherwise, that is

$$\mathsf{R}^T\mathsf{N} = \begin{pmatrix} 0 & 0 & 0 \\ 0 & |E| & 0 \\ 0 & 0 & |E| \end{pmatrix}. \tag{5.5}$$

Equivalence (5.5) can be checked also taking into account the algebraic expressions of N, R given in (5.1) and (5.2), respectively. Indeed, we have

$$\mathsf{R}^T\mathsf{N} = \begin{pmatrix} 0 & 0 & 0 \\ 0 & \frac{1}{2}\sum_{i=1}^m (x_i y_{i+1} - x_{i+1} y_i) & 0 \\ 0 & 0 & \frac{1}{2}\sum_{i=1}^m (x_i y_{i+1} - x_{i+1} y_i) \end{pmatrix},$$

which is indeed (5.5), taking into account the Shoelace formula, according to which the area of the polygon E (with sign) is given by

$$\frac{1}{2}\sum_{i=1}^m (x_i y_{i+1} - x_{i+1} y_i).$$

Finally, the matrix M is built as follows. Let

$$\mathsf{P} = \mathsf{I} - \mathsf{N}(\mathsf{N}^T\mathsf{N})^{-1}\mathsf{N}^T,$$

with I the $m \times m$ identity matrix. The matrix P is the projection matrix on the space orthogonal to the columns of N. Then, we set

$$\mathsf{M} = \frac{1}{|E|}\mathsf{R}\mathsf{R}^T + s\,\mathsf{P}\ , \tag{5.6}$$

with $s = \mathrm{trace}(\frac{1}{|E|}\mathsf{R}\mathsf{R}^T) > 0$ a scaling factor. Recalling (5.4) and the definition of P, it is easy to check that the above matrix M satisfies the consistency condition (5.3). Moreover, also the stability property (S2) can be proved, see for instance [9, 2].

We remark that, whenever the mesh is made of triangles, the matrix M coincides with the (elemental) finite element stiffness matrix, *i.e.*, on triangular elements the MFD and FEM methods are the same. Indeed, on the one hand, the projection matrix P turns out to be the null matrix, and the matrix M becomes:

$$\mathsf{M} = \frac{1}{|E|}\mathsf{R}\mathsf{R}^T = \frac{1}{4|E|}\begin{pmatrix} m_{11} & m_{12} & m_{13} \\ m_{21} & m_{22} & m_{23} \\ m_{31} & m_{32} & m_{33} \end{pmatrix},$$

where

$$\begin{aligned} m_{11} &= (x_2 - x_3)^2 + (y_2 - y_3)^2, \\ m_{12} = m_{21} &= -(x_1 - x_3)(x_2 - x_3) - (y_1 - y_3)(y_2 - y_3), \\ m_{13} = m_{31} &= (x_1 - x_2)(x_2 - x_3) + (y_1 - y_2)(y_2 - y_3), \\ m_{22} &= (x_1 - x_3)^2 + (y_1 - y_3)^2, \\ m_{23} = r_{32} &= -(x_1 - x_2)(x_1 - x_3) - (y_1 - y_2)(y_1 - y_3), \\ m_{33} &= (x_1 - x_2)^2 + (y_1 - y_2)^2. \end{aligned}$$

On the other hand, we recall that the Lagrangian finite element shape functions $\varphi_i(x, y)$, $i = 1, 2, 3$, can be written as

$$\begin{aligned} \varphi_1(x, y) &= \frac{1}{2|E|} \left[(x_2 y_3 - x_3 y_2) + (y_2 - y_3)x + (x_3 - x_2)y \right], \\ \varphi_2(x, y) &= \frac{1}{2|E|} \left[(x_3 y_1 - x_1 y_3) + (y_3 - y_1)x + (x_1 - x_3)y \right], \\ \varphi_3(x, y) &= \frac{1}{2|E|} \left[(x_1 y_2 - x_2 y_1) + (y_1 - y_2)x + (x_2 - x_1)y \right], \end{aligned}$$

and therefore

$$\begin{aligned} \nabla\varphi_1(x, y) &= \frac{1}{2|E|} \left(y_2 - y_3, x_3 - x_2 \right), \\ \nabla\varphi_2(x, y) &= \frac{1}{2|E|} \left(y_3 - y_1, x_1 - x_3 \right), \\ \nabla\varphi_3(x, y) &= \frac{1}{2|E|} \left(y_1 - y_2, x_2 - x_1 \right). \end{aligned}$$

Therefore, a straightforward calculation shows that the stiffness matrix V associated to the Lagrangian finite element shape functions has components

$$\mathsf{V}(i, j) := \int_E \nabla\varphi_j \cdot \nabla\varphi_i \, \mathrm{d}x = |E| (\nabla\varphi_i)^T \cdot (\nabla\varphi_j) = \mathsf{M}(i, j), \qquad i, j = 1, 2, 3.$$

6 Numerical results

This section is devoted to present some numerical computations to confirm the theoretical results of the previous sections.

We consider the domain $\Omega =]-1, 1[^2$. For a parameter $0 < r < 1$, we define the (continuous) load

$$f(x, y) := \begin{cases} -8(2x^2 + 2y^2 - r^2) & \text{if } \sqrt{x^2 + y^2} > r, \\ -8r^2(1 - x^2 - y^2 + r^2) & \text{if } \sqrt{x^2 + y^2} \leq r, \end{cases} \tag{6.1}$$

and the Dirichlet boundary data $g(x,y) := (x^2+y^2-r^2)^2$. We consider a constant obstacle $\psi(x,y) := 0$, so that the exact minimizer of model problem (2.1) is given by

$$u(x,y) := (\max\{x^2+y^2-r^2, 0\})^2; \tag{6.2}$$

cf. [27]. Figure 1 (left) depicts the minimizer u together with the obstacle ψ in the case $r = 0.7$. The obstacle problem has been solved numerically by the Projected Successive Over

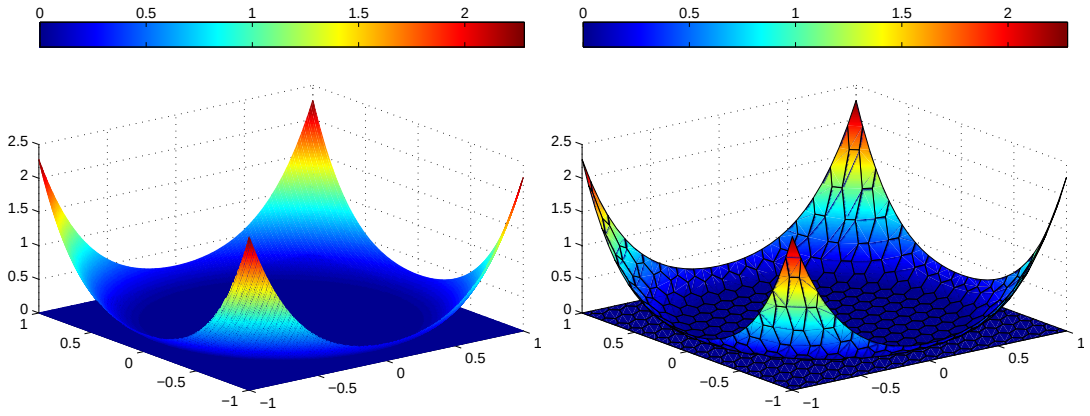

Figure 1: Left: exact minimizer u with the obstacle ψ ($r = 0.7$). Right: MFD minimizer u_h with the obstacle ψ ($r = 0.7$).

Relaxation (PSOR) method [16, 18, 21]. More precisely, we discretized the corresponding unconstrained problem (that is, the Poisson equation) by means of MFD method which reads in matrix form as $\mathsf{A}\widetilde{u}_h = \mathsf{f}$. Then, A is decomposed as $\mathsf{A} = \mathsf{D}+\mathsf{L}+\mathsf{U}$ for the projected Gauss-Seidel successive over-relaxation iteration (with over-relaxation parameter ω), and the minimizer u_h is found by constrained iteration up to a user-defined tolerance `TOL`. The *initial guess* is $\max\{\widetilde{u}_h, \psi\}$ where $\widetilde{u}_h$ is the solution to the unconstrained problem $\mathsf{A}\widetilde{u}_h = \mathsf{f}$. We refer to [18, 21] for more details. Throughout the section, the over-relaxation parameter ω has been chosen as $\omega = 1.75$, and the tolerance `TOL` in the iterative scheme is fixed equal to 10^{-9}.

We tested four different sequences of decompositions, that we denote by *triangular*, *quadrilateral*, *median-type 1* and *median-type 2*. An example of two consecutive levels of all the considered decomposition is shown in Figure 2. An example of MFD minimizer together with the obstacle ψ on a *median-type 1* polygonal mesh is shown in Figure 1 (right).

In Table 1 we report the computed (relative) errors $\varepsilon^r_{1,h}(u^I, u_h)$ in the discrete energy norm defined in (3.2), *i.e.*,

$$\varepsilon^r_{1,h}(u^I, u_h) = \frac{\|u^I - u_h\|_{1,h}}{\|u^I\|_{1,h}},$$

for the sequence of triangular and quadrilateral decompositions. Here and in the following, n_P denotes the number of polygons of the decomposition. In the last row of

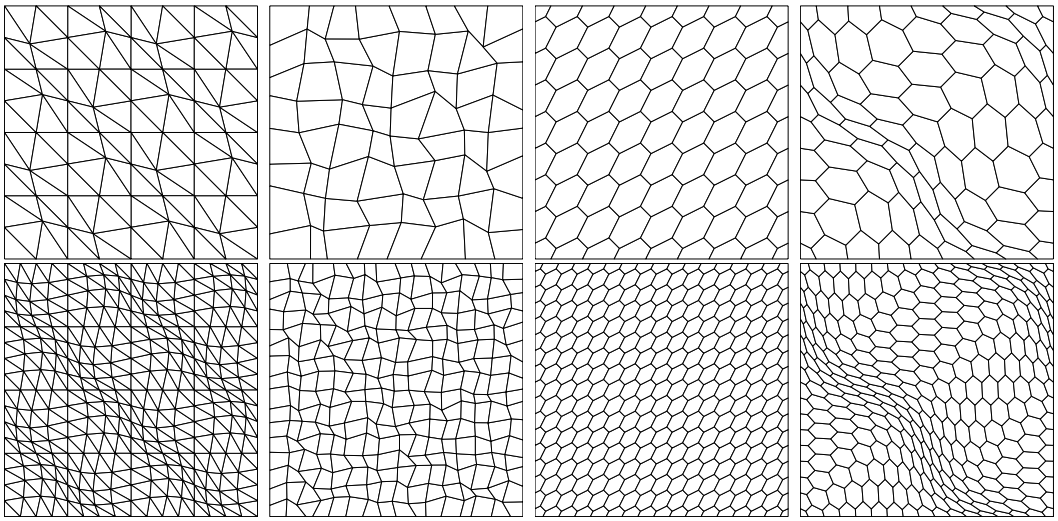

Figure 2: Two samples of the considered decompositions of $\Omega =]-1,1[^2$: one coarser (top) and one finer (bottom). From left to right: *triangular* mesh, *quadrilateral* mesh and *median-type 1*, *median-type 2* polygonal meshes.

Table 1 we also report the computed convergence rates obtained by the linear regression algorithm. We can observe that on quadrilateral meshes the computed convergence rate is linear as predicted by Theorem 4.1, whereas on triangular decomposition convergence is achieved slightly better that expected; such a behaviour has been already observed in [2]. The analogous results obtained on *median-type 1* and *median-type 2* decompositions

Table 1: Computed relative errors $\varepsilon^r_{1,h}(u^I, u_h)$ on the sequence of triangular and quadrilateral meshes.

triangular meshes		*quadrilateral meshes*	
n_P	$\varepsilon^r_{1,h}(u^I, u_h)$	n_P	$\varepsilon^r_{1,h}(u^I, u_h)$
128	3.7452e-02	64	6.4114e-02
512	1.1865e-02	256	2.5172e-02
2048	3.4448e-03	1024	1.2802e-02
8192	9.5227e-04	4096	6.7499e-03
32768	2.7586e-04	16384	3.4652e-03
rate	1.7809		1.0318

are shown in Figure 3 (loglog scale), and are indeed in agreement with our theoretical

estimates. Next, we also investigate the (relative) error behaviour in the discrete L^2- and

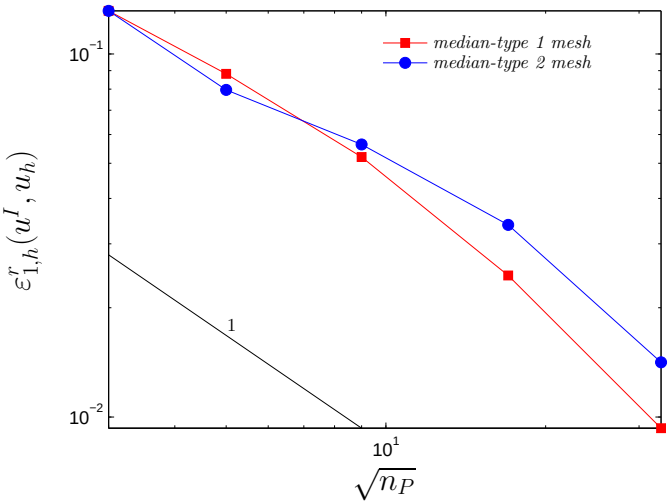

Figure 3: Computed relative errors $\varepsilon^r_{1,h}(u^I, u_h)$ versus the square root of the number of cells (loglog scale): *median-type 1* and *median-type 2* meshes.

L^∞-type norms defined in (3.3). To this aim, we set

$$\varepsilon^r_{0,h}(u^I, u_h) := \frac{\|u^I - u_h\|_{0,h}}{\|u^I\|_{0,h}}, \qquad \varepsilon^r_{\infty,h}(u^I, u_h) := \frac{\|u^I - u_h\|_{\infty,h}}{\|u^I\|_{\infty,h}}.$$

The computed errors $\varepsilon^r_{0,h}(u^I, u_h)$ and $\varepsilon^r_{\infty,h}(u^I, u_h)$ versus the square root of the number of cells are reported in Figure 4 (loglog scale). Results reported in Figure 4(a) refer to *triangular* and *quadrilateral* meshes, whereas results obtained on *median-type 1* and *median-type 2* decompositions are shown in Figure 4(b). A quadratic convergence rate is clearly observed.

Next, we compare the performance of MFD and FEM, and we investigate the effects of employing the discrete norms (3.2) and (3.3) instead of their continuous counterparts (that is, the $H^1(\Omega)$ and $L^2(\Omega)$ norms). First, we employ the FEM to approximate the model problem under consideration on a sequence of *triangular* decompositions, and computed the (relative) errors both in the $H^1(\Omega)$ seminorm and in the $L^2(\Omega)$ norm

$$\varepsilon^r_1(u^I, u_h) := \frac{|u^I - u_h|_{H^1(\Omega)}}{|u^I|_{H^1(\Omega)}}, \quad \varepsilon^r_0(u^I, u_h) := \frac{\|u^I - u_h\|_{L^2(\Omega)}}{\|u^I\|_{L^2(\Omega)}}. \tag{6.3}$$

To compute the right-hand side of the Finite Element variational formulation, we have employed the barycenter quadrature formula, which is exact for linear polynomials, and therefore it is consistent with the quadrature formula (3.7). In Table 2 we compare the Finite Element relative errors computed as in (6.3) with their discrete counterpart, namely $\varepsilon^r_{1,h}(u^I, u_h)$ and $\varepsilon^r_{0,h}(u^I, u_h)$. We clearly observe that, for both $s = 0$ and $s = 1$, the relative error $\varepsilon^r_{s,h}(u^I, u_h)$ (which only employs nodal values) is systematically smaller

(a) *Triangular* and *quadrilateral* meshes.

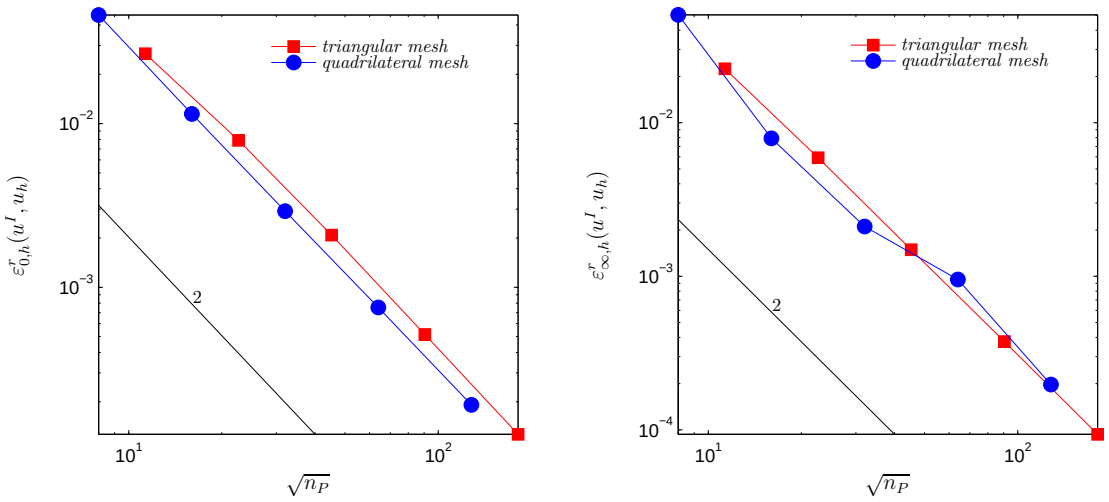

(b) *Median* meshes.

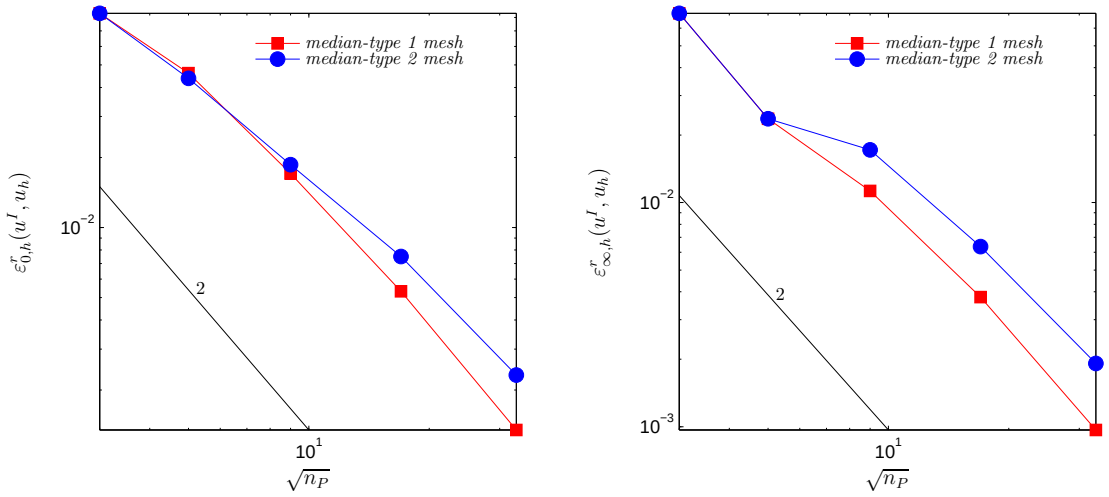

Figure 4: Computed relative errors $\varepsilon^r_{0,h}(u^I, u_h)$ (left) and $\varepsilon^r_{\infty,h}(u^I, u_h)$ (right) versus the square root of the number of cells (loglog scale).

than $\varepsilon^r_s(u^I, u_h)$. This phenomenon is probably related to an improved accuracy in the nodal value approximation. Next, we compare results obtained by MFD and FEM. In Figure 5 we plot the computed errors $\varepsilon^r_{s,h}(u^I, u_h)$, $s = 0, 1$, versus the square root of the number of cells. We observe that both MFD and FEM achieve asymptotic convergence at a rate slightly bigger than predicted by our theoretical estimates, and that MFD produces a larger error. However, the total cost-accuracy should take into account that the FEM is more expensive in terms of computational costs due to the numerical integration.

Table 2: Finite Element approximation: comparison between discrete and continuous norms, namely $\varepsilon^r_{s,h}(u^I, u_h)$ and $\varepsilon^r_s(u^I, u_h)$, $s = 0, 1$.

n_P	$\varepsilon^r_1(u^I, u_h)$	$\varepsilon^r_{1,h}(u^I, u_h)$	$\varepsilon^r_0(u^I, u_h)$	$\varepsilon^r_{0,h}(u^I, u_h)$
128	2.4692e-01	1.7761e-02	2.0321e-01	1.1906e-02
512	1.2123e-01	7.8972e-03	4.8759e-02	4.6443e-03
2048	6.0299e-02	2.3997e-03	1.2071e-02	1.2427e-03
8192	3.0113e-02	7.3530e-04	3.0086e-03	3.1091e-04
32768	1.5052e-02	2.3510e-04	7.5225e-04	7.7263e-05
rate	1.0081	1.5903	2.0174	1.8436

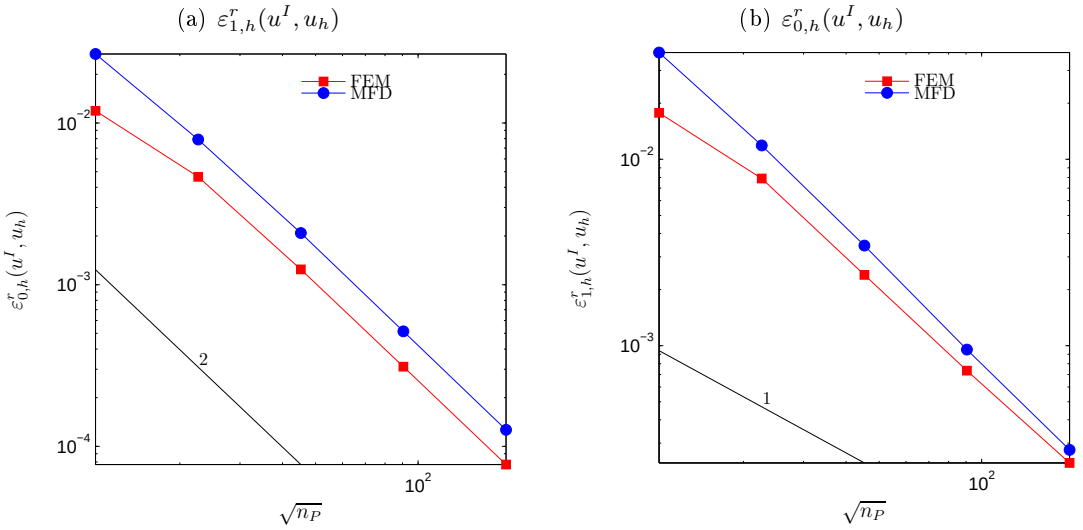

Figure 5: Comparison between FEM and MFD: computed relative errors $\varepsilon^r_{s,h}(u^I, u_h)$, $s = 0, 1$, versus the square root of the number of cells (loglog scale).

Finally, we present some numerical computations to confirm that the theoretical results of the previous sections are valid also on non-convex domains (cf. Remark 4.1). To this aim we choose the L-shaped domain $\Omega =]-1, 1[^2 \setminus [0, 1]^2$, and we consider the same test problem as before. Figure 6 (right) shows a plot of the MFD minimizer u_h together with the obstacle ψ ($r = 0.7$). We tested the MFD method on a sequence of *quadrilateral* meshes: a sample is shown in Figure 6 (left). The computed relative errors $\varepsilon^r_{1,h}(u^I, u_h)$ and $\varepsilon^r_{0,h}(u^I, u_h)$ are reported in Figure 7 (loglog scale): as predicted by Theorem 4.1, we observe a linear convergence rate in the discrete energy norm. We also observe that the

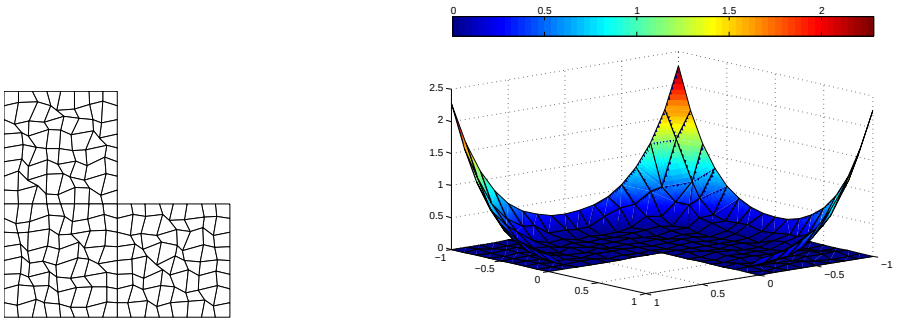

Figure 6: L-shaped domain: a sample of the *quadrilateral* decomposition (left), and the corresponding MFD minimizer u_h together with the obstacle ψ (right).

relative error in the discrete L^2 norm tends to zero quadratically as the mesh is refined.

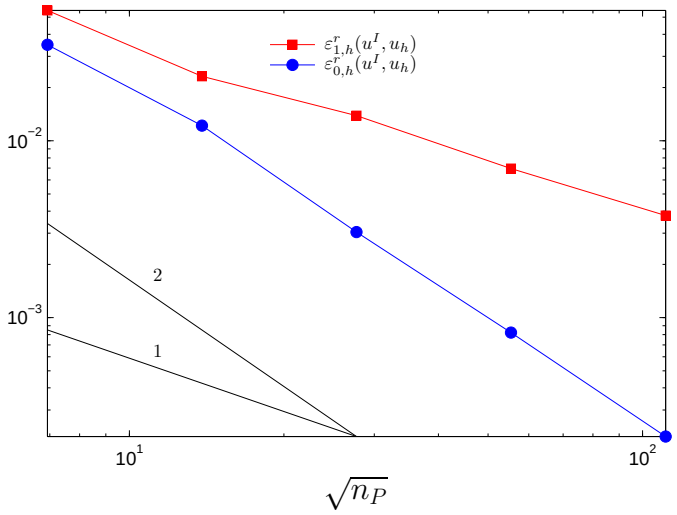

Figure 7: L-shaped domain: computed relative errors $\varepsilon^r_{1,h}(u^I, u_h)$ and $\varepsilon^r_{0,h}(u^I, u_h)$ versus the square root of the number of cells (loglog scale).

Acknowledgments

We are grateful to Gianmarco Manzini for the help in generating polygonal median meshes.

References

[1] L. Beirão da Veiga. A mimetic finite difference method for linear elasticity, 2010. In press on *M2AN Math. Model. Numer. Anal.*, doi 10.1051/m2an/2010001.

[2] L. Beirão da Veiga, V. Gyrya, K. Lipnikov, and G. Manzini. Mimetic finite difference method for the Stokes problem on polygonal meshes. *J. Comput. Phys*, 228:7215–7232, 2009.

[3] L. Beirão da Veiga, K. Lipnikov, and G. Manzini. Convergence analysis of the high-order mimetic finite difference method. *Numer. Math.*, 113(3):325–356, 2009.

[4] L. Beirão da Veiga and G. Manzini. An a posteriori error estimator for the mimetic finite difference approximation of elliptic problems. *Int. J. Numer. Methods Engrg.*, 76(11):1696–1723, 2008.

[5] L. Beirão da Veiga and D. Mora. A mimetic discretization of the Reissner-Mindlin plate bending problem. Submitted for publication.

[6] S. Brenner and L. Scott. *The Mathematical Theory of Finite Element Methods*. Springer-Verlag, Berlin/Heidelberg, 1994.

[7] H. Brezis. Problèmes unilatéraux. Thése d'etat. *J. Math. Pures. Appl.*, IX, Ser. 72:1–168, 1971.

[8] H. Brezis and G. Stampacchia. Sur la régularité de la solution d'inéquations elliptiques. *Bull. Soc. Math. France*, 96:153–180, 1968.

[9] F. Brezzi, A. Buffa, and K. Lipnikov. Mimetic finite differences for elliptic problems. *M2AN Math. Model. Numer. Anal.*, 43(2):277–295, 2009.

[10] F. Brezzi, W.W. Hager, and P.A. Raviart. Error estimates for the finite element solution of variational inequalities. *Numer. Math.*, 28:431–443, 1977.

[11] F. Brezzi, K. Lipnikov, and M. Shashkov. Convergence of the mimetic finite difference method for diffusion problems on polyhedral meshes. *SIAM J. Numer. Anal.*, 43(5):1872–1896, 2005.

[12] F. Brezzi, K. Lipnikov, M Shashkov, and V. Simoncini. A new discretization methodology for diffusion problems on generalized polyhedral meshes. *Comput. Methods Appl. Mech. Engrg.*, 196(37-40):3682–3692, 2007.

[13] F. Brezzi, K. Lipnikov, and V. Simoncini. A family of mimetic finite difference methods on polygonal and polyhedral meshes. *Math. Models Methods Appl. Sci.*, 15(10):1533–1551, 2005.

[14] A. Cangiani and G. Manzini. Flux reconstruction and pressure post-processing in mimetic finite difference methods. *Comput. Methods Appl. Mech. Engrg.*, 197(9-12):933–945, 2008.

[15] P. G. Ciarlet. *The Finite Element Method for Elliptic Problems.* North-Holland, Amsterdam, 1978.

[16] C. W. Cryer. Successive overrelaxation methods for solving linear complementarity problems arising from free boundary problems. In *Free boundary problems, Vol. I (Pavia, 1979)*, pages 109–131. Ist. Naz. Alta Mat. Francesco Severi, Rome, 1980.

[17] T. Dupont and R. Scott. Polynomial approximation of functions in Sobolev spaces. *Math. Comp.*, 34(150):441–463, 1980.

[18] C. M. Elliott and J. R. Ockendon. *Weak and variational methods for moving boundary problems*, volume 59 of *Research Notes in Mathematics.* Pitman (Advanced Publishing Program), Boston, Mass., 1982.

[19] R. S. Falk. Error estimates for the approximation of a class of variational inequalities. *Math. Comput.*, 28:963–971, 1974.

[20] A. Friedman. *Variational principles and free-boundary problems.* Pure and Applied Mathematics. John Wiley & Sons Inc., New York, 1982. A Wiley-Interscience Publication.

[21] R. Glowinski, J.-L. Lions, and R. Trémolières. *Numerical analysis of variational inequalities*, volume 8 of *Studies in Mathematics and its Applications*. North-Holland Publishing Co., Amsterdam, 1981. Translated from the French.

[22] P. Jaillet, D. Lamberton, and B. Lapeyre. Variational inequalities and the pricing of American options. *Acta Appl. Math.*, 21(3):263–289, 1990.

[23] D. Kinderlehrer and G. Stampacchia. *An introduction to variational inequalities and their applications*, volume 31 of *Classics in Applied Mathematics*. Society for Industrial and Applied Mathematics (SIAM), Philadelphia, PA, 2000. Reprint of the 1980 original.

[24] H. Lewy and G. Stampacchia. On the regularity of the solution of a variational inequality. *Comm. Pure Appl. Math.*, 22:153–188, 1969.

[25] K. Lipnikov, J.D. Moulton, and D. Svyatskiy. A Multilevel Multiscale Mimetic (M^3) method for two-phase flows in porous media. *J. Comp. Phys.*, 227:6727–6753, 2008.

[26] K. Lipnikov, M. Shashkov, and I. Yotov. Local flux mimetic finite difference methods. *Numer. Math.*, 112(1):115–152, 2009.

[27] R. H. Nochetto, K. G. Siebert, and A. Veeser. Pointwise a posteriori error control for elliptic obstacle problems. *Numer. Math.*, 95(1):163–195, 2003.

Appendix A: convergence result in the case of homogeneous boundary conditions

This section is devoted to show that, if we restrict ourselves to the case of homogeneous boundary conditions, Theorem 4.1 can be proved in a much simpler way, following the idea proposed in [19]. For the sake of completeness we restate Theorem 4.1, and report the proof.

Theorem 6.1. *Let $u \in K \cap H^2(\Omega)$ be the solution to the continuous problem* (2.1) *with homogeneous boundary conditions,* i.e., *$g = 0$, and let $u_h \in K_h$ be the corresponding mimetic approximation, obtained by solving the discrete problem* (3.8). *Then, it holds*

$$\|u_h - u_I\|_{1,h} \leq Ch,$$

where the constant C is independent of the mesh-size h.

Proof. We set $e_h := u_h - u_\mathrm{I}$ and $u^1 := I^1 u$, where I^1 is the Lagrangian interpolation operator onto the space of continuous piecewise linear functions defined on Ω_h. By using

(S1)-(S2), we get

$$
\begin{aligned}
c_1\|e_h\|_{1,h}^2 &\leq a_h(e_h,e_h)\\
&\leq (f,e_h)_h - a_h(u_{\mathrm{I}},e_h)\\
&\leq (f,e_h)_h - a_h(u_{\mathrm{I}}-(u^1)_{\mathrm{I}},e_h) - a_h((u^1)_{\mathrm{I}},e_h)\\
&\leq (f,e_h)_h + c_2\|u_{\mathrm{I}}-(u^1)_{\mathrm{I}}\|_{1,h}\|e_h\|_{1,h} - \sum_{E\in\Omega_h}\sum_{\mathsf{e}\in\mathcal{E}_h^E}\frac{\partial u^1}{\partial n}\int_e R_h^E e_h\,\mathrm{d}x\\
&\leq (f,e_h)_h + c_2\|u_{\mathrm{I}}-(u^1)_{\mathrm{I}}\|_{1,h}\|e_h\|_{1,h} - \sum_{E\in\Omega_h}\int_E \nabla R_h^E e_h\cdot\nabla u^1\,\mathrm{d}x \qquad (6.4)\\
&\leq (f,e_h)_h + c_2\|u_{\mathrm{I}}-(u^1)_{\mathrm{I}}\|_{1,h}\|e_h\|_{1,h}\\
&\quad + \sum_{E\in\Omega_h}\int_E \nabla R_h^E(u_h-u_{\mathrm{I}})\cdot\nabla(u-u^1)\,\mathrm{d}x\\
&\quad - \sum_{E\in\Omega_h}\int_E \nabla R_h^E(u_h-u_{\mathrm{I}})\cdot\nabla u\,\mathrm{d}x.
\end{aligned}
$$

Let us preliminary estimate the term $\|(u-u^1)_{\mathrm{I}}\|_{1,h}$. For simplicity, we set $v=u-u^1$. Using definition (3.2) of the norm $\|\cdot\|_{1,h}$ and the Cauchy-Schwarz inequality, we get

$$
\begin{aligned}
\|v_{\mathrm{I}}\|_{1,h}^2 &= \sum_{E\in\Omega_h}|E|\sum_{\mathsf{e}\in\mathcal{E}_h^E}\left[\frac{1}{|\mathsf{e}|}\left(v^{\mathsf{v}_2}-v^{\mathsf{v}_1}\right)\right]^2 = \sum_{E\in\Omega_h}|E|\sum_{\mathsf{e}\in\mathcal{E}_h^E}\left[\frac{1}{|\mathsf{e}|}\int_{\mathsf{e}} v'ds\right]^2\\
&\leq \sum_{E\in\Omega_h}|E|\sum_{\mathsf{e}\in\mathcal{E}_h^E}\left[\frac{1}{|\mathsf{e}|}\|\nabla v\|_{L^2(\mathsf{e})}^2\right].
\end{aligned}
$$

Applying the trace inequality (3.1) to ∇v and employing a standard interpolation error estimate yield

$$
\|(u-u^1)_{\mathrm{I}}\|_{1,h}^2 \lesssim \sum_{E\in\Omega_h}\left[\|\nabla(u-u^1)\|_{L^2(E)}^2 + h_E^2\,|u|_{H^2(E)}^2\right] \lesssim h^2\,|u|_{H^2(\Omega)}^2\,. \qquad (6.5)
$$

From (6.4), by the employing Young inequality combined with (6.5), we get

$$
\begin{aligned}
\|e_h\|_{1,h}^2 \lesssim (f,e_h)_h + h^2\,|u|_{H^2(\Omega)}^2 &+ \sum_{E\in\Omega_h}\int_E \nabla R_h^E(u_h-u_{\mathrm{I}})\cdot\nabla(u-u^1)\,\mathrm{d}x\\
&- \sum_{E\in\Omega_h}\int_E \nabla R_h^E(u_h-u_{\mathrm{I}})\cdot\nabla u\,\mathrm{d}x.
\end{aligned}
$$

Moreover, for an arbitrary element v of the space K, integration by parts and the Cauchy-Schwarz inequality yield

$$
\begin{aligned}
\|e_h\|_{1,h}^2 \lesssim \quad & (f,e_h)_h + h^2\,|u|_{H^2(\Omega)}^2 + \|\nabla R_h^E(u_h-u_{\rm I})\|_{L^2(\Omega)}\|\nabla(u-u^1)\|_{L^2(\Omega)} \\
& - \sum_{E\in\Omega_h}\int_E \nabla(u-R_h^E u_{\rm I})\cdot\nabla u\,{\rm d}x + \sum_{E\in\Omega_h}\int_E \nabla(u-R_h^E u_h)\cdot\nabla u\,{\rm d}x \\
\lesssim \quad & (f,e_h)_h + h^2\,|u|_{H^2(\Omega)}^2 + \|\nabla R_h^E(u_h-u_{\rm I})\|_{L^2(\Omega)}\|\nabla(u-u^1)\|_{L^2(\Omega)} \\
& + \|\Delta u\|_{L^2(\Omega)}\|u-R_h^E u_{\rm I}\|_{L^2(\Omega)} - \sum_{E\in\Omega_h}\int_E \nabla(v-u)\cdot\nabla u\,{\rm d}x \\
& + \sum_{E\in\Omega_h}\int_E \nabla(v-R_h^E u_h)\cdot\nabla u\,{\rm d}x \\
\lesssim \quad & (f,e_h)_h + h^2\,|u|_{H^2(\Omega)}^2 + \|\nabla R_h^E(u_h-u_{\rm I})\|_{L^2(\Omega)}\|\nabla(u-u^1)\|_{L^2(\Omega)} \\
& + \|\Delta u\|_{L^2(\Omega)}\|u-R_h^E u_{\rm I}\|_{L^2(\Omega)} - \int_\Omega f(v-u)\,{\rm d}x \\
& + \|v-R_h^E u_h\|_{L^2(\Omega)}\|\Delta u\|_{L^2(\Omega)},
\end{aligned}
$$

where in the last inequality we have employed (2.1). Finally, a simple manipulation of the terms appearing in the above inequality gives the following

$$
\begin{aligned}
\|e_h\|_{1,h}^2 \lesssim & \Big\{(f,e_h)_h - (f,R_h^E e_h)\Big\} + \Big\{(f,R_h^E e_h) - (f,v-u)\Big\} \\
& + h^2\,|u|_{H^2(\Omega)}^2 + \|\nabla R_h^E(u_h-u_{\rm I})\|_{L^2(\Omega)}\|\nabla(u-u^1)\|_{L^2(\Omega)} \\
& + \|\Delta u\|_{L^2(\Omega)}\Big(\|u-R_h^E u_{\rm I}\|_{L^2(\Omega)} + \|v-R_h^E u_h\|_{L^2(\Omega)}\Big) \\
\lesssim & \Big\{(f,e_h)_h - (f,R_h^E e_h)\Big\} + \Big\{(f,R_h^E u_h - v) + (f,u-R_h^E u_{\rm I})\Big\} \\
& + h^2|u|_{H^2(\Omega)}^2 + \|\nabla R_h^E(u_h-u_{\rm I})\|_{L^2(\Omega)}\|\nabla(u-u^1)\|_{L^2(\Omega)} \\
& + \|\Delta u\|_{L^2(\Omega)}\Big(\|u-R_h^E u_{\rm I}\|_{L^2(\Omega)} + \|v-R_h^E u_h\|_{L^2(\Omega)}\Big) \qquad (6.6) \\
\lesssim & \Big\{(f,e_h)_h - (f,R_h^E e_h)\Big\} \\
& + \Big(\|f\|_{L^2(\Omega)} + \|\Delta u\|_{L^2(\Omega)}\Big)\Big(\|v-R_h^E u_h\|_{L^2(\Omega)} + \|u-R_h^E u_{\rm I}\|_{L^2(\Omega)}\Big) \\
& + h^2\,|u|_{H^2(\Omega)}^2 + \|\nabla R_h^E(u_h-u_{\rm I})\|_{L^2(\Omega)}\|\nabla(u-u^1)\|_{L^2(\Omega)} \\
\lesssim & \Big\{(f,e_h)_h - (f,R_h^E e_h)\Big\} + \|v-R_h^E u_h\|_{L^2(\Omega)} + \|u-R_h^E u_{\rm I}\|_{L^2(\Omega)} \\
& + h^2\,|u|_{H^2(\Omega)}^2 + \|\nabla R_h^E(u_h-u_{\rm I})\|_{L^2(\Omega)}\|\nabla(u-u^1)\|_{L^2(\Omega)},
\end{aligned}
$$

where in the last inequality we used that $f,\Delta u\in L^2(\Omega)$.

By using (4.7) and proceeding as in the estimate of the *First Piece* in [9], it is easy to check that there holds

$$
\big|(f,e_h)_h - (f,R_h^E e_h)\big| \lesssim h\|f\|_{L^2(\Omega)}\|e_h\|_{1,h}. \qquad (6.7)
$$

From (6.6), by employing the Young inequality combined with (6.7), we get

$$\begin{aligned}\|e_h\|_{1,h}^2 \lesssim h^2 &+ \|v - R_h^E u_h\|_{L^2(\Omega)} + \|u - R_h^E u_{\mathrm{I}}\|_{L^2(\Omega)} \\ &+ \|\nabla R_h^E (u_h - u_{\mathrm{I}})\|_{L^2(\Omega)} \|\nabla (u - u^1)\|_{L^2(\Omega)}.\end{aligned}$$

Using assumption (L4) and a standard interpolation error estimate together with Young inequality yields

$$\|e_h\|_{1,h}^2 \lesssim h^2 + \inf_{v \in K} \|v - R_h^E u_h\|_{L^2(\Omega)} + \|u - R_h^E u_{\mathrm{I}}\|_{L^2(\Omega)}. \tag{6.8}$$

Moreover, by applying inequality (4.6) we get

$$\|e_h\|_{1,h}^2 \lesssim h^2 + \inf_{v \in K} \|v - R_h^E u_h\|_{L^2(\Omega)}. \tag{6.9}$$

In order to estimate the term $\inf_{v \in K} \|R_h^E u_h - v\|_{L^2(\Omega)}$, we mimick the proof in [19] and we introduce the function u^* with

$$u^*_{|E} = \max\{R_h^E u_h, \psi_{|E}\}$$

for every $E \in \Omega_h$, so that the inequality $u^* \geq \psi$ holds in Ω. It is possible to prove that $R_h^E u_h, \psi \in H^1(\Omega)$ implies $u^* \in H^1(\Omega)$ (see *e.g.* [24]). Finally, the condition $\psi \leq 0$ on Γ yields that $u^* \in H_0^1(\Omega)$. Thus the function u^* is an element of the set K. Let

$$\Lambda_h = \{x \in \Omega : \quad R_h^E u_h < \psi\},$$

so that

$$\|R_h^E u_h - u^*\|_{L^2(\Omega)} = \int_{\Lambda_h} |R_h^E u_h - \psi|^2 \, \mathrm{d}x,$$

since $R_h^E u_h - u^* = 0$ on $\Omega \setminus \Lambda_h$. As for every $\mathsf{v} \in \mathcal{N}_h$ there holds $u_h(\mathsf{v}) \geq \psi_{\mathrm{I}}(\mathsf{v})$, employing assumption (L6) yields

$$R_h^E u_h - R_h^E \psi_{\mathrm{I}} \geq 0 \quad \text{in } \Omega.$$

Consequently, for every $x \in \Lambda_h$ there holds

$$0 < |(\psi - R_h^E u_h)(x)| = (\psi - R_h^E u_h)(x) \leq (\psi - R_h^E \psi_{\mathrm{I}})(x) = |(\psi - R_h^E \psi_{\mathrm{I}})(x)|,$$

and thus,

$$\|R_h^E u_h - u^*\|_{L^2(\Omega)}^2 = \int_{\Lambda_h} |R_h^E u_h - \psi|^2 \, \mathrm{d}x \leq \int_{\Lambda_h} |\psi - R_h^E \psi_{\mathrm{I}}|^2 \, \mathrm{d}x \leq \|\psi - R_h^E \psi_{\mathrm{I}}\|_{L^2(\Omega)}^2.$$

Therefore, by using (4.6) and $\psi \in H^2(\Omega)$, we obtain

$$\|R_h^E u_h - u^*\|_{L^2(\Omega)} \lesssim \|\psi - R_h^E \psi_{\mathrm{I}}\|_{L^2(\Omega)} \lesssim h^2 \, |\psi|_{H^2(\Omega)}. \tag{6.10}$$

Combining (6.10) and (6.9) yields the thesis. □

MOX Technical Reports, last issues

Dipartimento di Matematica "F. Brioschi",
Politecnico di Milano, Via Bonardi 9 - 20133 Milano (Italy)

14/2010 Paola F. Antonietti, Lourenco Beirão da Veiga, Marco Verani:
A Mimetic Discretization of Elliptic Obstacle Problems

13/2010 G.M. Porta, Simona Perotto, F. Ballio:
A Space-Time Adaptation Scheme for Unsteady Shallow Water Problems

12/2010 Riccardo Sacco, Paola Causin, Paolo Zunino, Manuela T. Raimondi:
A multiphysics/multiscale numerical simulation of scaffold-based cartilage regeneration under interstitial perfusion in a bioreactor

11/2010 Paolo Biscari, Sara Minisini, Dario Pierotti, Gianmaria Verzini, Paolo Zunino:
Controlled release with finite dissolution rate

10/2010 Alfio Quarteroni, Ricardo Ruiz Baier:
Analysis of a finite volume element method for the Stokes problem

09/2010 Laura M. Sangalli, Piercesare Secchi, Simone Vantini, Valeria Vitelli:
Joint Clustering and Alignment of Functional Data: an Application to Vascular Geometries

08/2010 Francesca Ieva, Anna Maria Paganoni:
Multilevel models for clinical registers concerning STEMI patients in a complex urban reality: a statistical analysis of MOMI^2 survey

07/2010 Laura M. Sangalli, Piercesare Secchi, Simone Vantini, Valeria Vitelli:
Functional clustering and alignment methods with applications

06/2010 Jordi Alastruey, Tiziano Passerini, Luca Formaggia, Joaquim Peiró:
The effect of visco-elasticity and other physical properties on aortic and cerebral pulse waveforms: an analytical and numerical study

05/2010 Matteo Longoni, A.C.I. Malossi, Alfio Quarteroni, Andrea Villa:
A complete model for non-Newtonian sedimentary basins in presence of faults and compaction phenomena